Mixed Control for 2-D Markov Jump Systems with Multiaccess Stochastic Communication Protocol

Yu Zhang, Qing Chen, Chengyi Han, Taiping Jiang, Yebin Chen

***Abstract*—This paper addresses the mixed $\mathcal{H}_\infty/\mathcal{L}_2-\mathcal{L}_\infty$ control problem for two-dimensional (2-D) Markov jump systems using a multiaccess stochastic communication protocol (MSCP). The actuators are randomly selected, allowing only some of the actuator nodes to access the communication network channels. Two independent Markov chains govern the switching of plant modes and actuator access states. A state-feedback controller is formulated based on the MSCP and a hidden Markov model. We derive a sufficient condition such that the closed-loop 2-D system is stochastically stable and satisfies $\mathcal{H}_\infty/\mathcal{L}_2-\mathcal{L}_\infty$ mixed performance employing Lyapunov's direct method and Schur's complement. Then, we develop a numerically efficient strategy to determine the desired controller gains of the state-feedback controller. Finally, we demonstrate the effectiveness of the proposed controller through a numerical example based on the Darboux equation.**

***Index Terms*—Two-dimensional system, Markov jump system, mixed control, stochastic communication protocol.**

I. Introduction

OVER the years, two-dimensional (2-D) systems have stimulated research interests in different application scenarios, such as gas filtration process [1], motion systems [2], and image data analysis [3]. Several extensively used mathematical models have been developed to describe 2-D systems, with the Roesser [4] and the Fornasini-Marchesini [5] models being the most familiar. Compared to one-dimensional systems, 2-D systems significantly increase the complexity of analysis and calculation due to the coordinated evolution of their states in multiple directions. In some 2-D systems, internal parameters or structures may change suddenly due to various widespread uncertainties. This phenomenon can be effectively characterized using Markov stochastic processes. Therefore, 2-D Markov jump systems (MJSs), as a typical hybrid system, have never stopped being discussed. Wu et al. [6] considered the problem of asynchronous $\mathcal{H}_\infty$ control for 2-D MJSs. Ghous et al. [7] studied the stochastic stability and control problem of 2-D continuous delayed MJSs. Zhu et al. [8] focused on 2-D discrete-time hidden MJSs subject to partly known mode-observation conditional probabilities and presented state feedback controller design schemes. In Refs. [6–8], $\mathcal{H}_\infty$ performance performance is considered as the primary control objective. However, in actual industry, there is also a requirement to restrict the peak value of the system output [9], necessitating the consideration of mixed $\mathcal{H}_\infty/\mathcal{L}_2-\mathcal{L}_\infty$ control.

In real-world networks, bandwidth and data rates are often limited [10, 11], so only a portion of the signals can be transmitted simultaneously between system components (e.g., sensors, controllers, and actuators) to avoid data conflicts. Furthermore, for different transmission mediums, the signals may interfere with each other during the propagation process, thus limiting the channel's ability to accommodate and transmit multiple node data simultaneously. Therefore, effective access scheduling of nodes is critical to save communication resources and avoid data congestion. To solve this problem, an effective approach is to determine which actuator nodes should access the communication network through communication protocols. For instance, in [12], the round-robin protocol is used to schedule the data transmission order of the controller-actuator (C/A) channel to select transmission nodes periodically. In [13, 14], the system schedules transmissions based on the deviation between the current and the previous state, and this method is known as the weighted try-once-discard protocol. In addition, in [15, 16], the stochastic communication protocol selects transmission nodes based on a random process. A communication protocol based on a discrete-time Markov chain is presented to schedule nodes in [17], which can determine which component node accesses the communication network [18, 19]. The common feature of the above protocols is that at any instant, only one node is allowed to access the communication channel to send or receive information. Although conventional protocols restrict single-node access, under certain specific network conditions, multiple nodes may also communicate simultaneously [20].

Inspired by the above discussion, this paper considers the mixed $\mathcal{H}_\infty/\mathcal{L}_2-\mathcal{L}_\infty$ control problem for 2-D MJS with a multiaccess stochastic communication protocol (MSCP), where multiple actuator nodes are selected to transmit signals in the communication channel. Mapping the plant mode switching and the actuator access state to a new Markov chain can effectively facilitate control design and analysis. The problem to be solved is to design a state feedback controller such that the resulting closed-loop system is stochastically stable (SS) and satisfies $\mathcal{H}_\infty/\mathcal{L}_2-\mathcal{L}_\infty$ mixed performance. A sufficient condition for the stochastic stability and $\mathcal{H}_\infty/\mathcal{L}_2-\mathcal{L}_\infty$ mixed performance of the closed-loop 2-D MJS is established using Lyapunov's direct method and Schur's complement. Then, the state feedback controller is designed by introducing the relaxation matrix. Finally, the effectiveness of the proposed analysis and synthesis results is verified by taking the Darboux equation as an example.

Manuscript received May 10, 2024; revised October 9, 2024.

Yu Zhang is a postgraduate student at the School of Computer Science and Technology, Anhui University of Technology, Ma'anshan 243032, China (e-mail: yzhang@ahut.edu.cn).

Qing Chen is a postgraduate student at the School of Computer Science and Technology, Anhui University of Technology, Ma'anshan 243032, China (e-mail: chenqing@ahut.edu.cn).

Chengyi Han is a postgraduate student at the School of Computer Science and Technology, Anhui University of Technology, Ma'anshan 243032, China (e-mail: hanchengyi@ahut.edu.cn).

Taiping Jiang is an associate professor at the School of Computer Science and Technology, Anhui University of Technology, Ma'anshan 243032, China (corresponding author, e-mail: tpjiang2008@163.com).

Yebin Chen is an full professor at the School of Computer Science and Technology, Anhui University of Technology, Ma'anshan 243032, China (e-mail: chenyb@ahut.edu.cn).

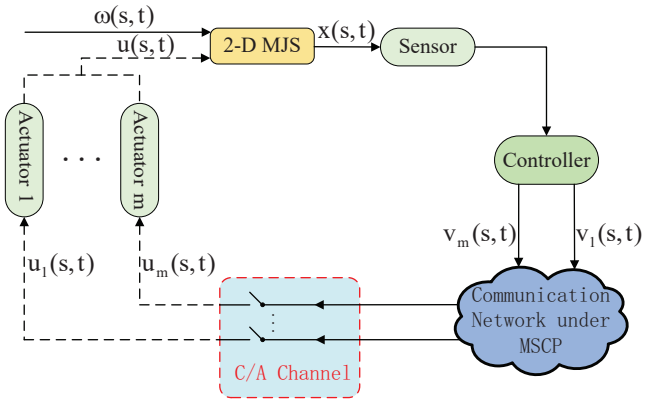

Fig. 1. System structure with communication network

II. Preliminaries

A. Model description

Consider a class of 2-D MJS described by

$$\begin{cases} x^1(s,t) = A(\rho_{s,t})x(s,t) + B(\rho_{s,t})u(s,t) + D(\rho_{s,t})\omega(s,t), \\ y(s,t) = C(\rho_{s,t})x(s,t), \end{cases} \tag{1}$$

where

$$x^1(s,t) = \begin{bmatrix} x^h(s+1,t) \\ x^v(s,t+1) \end{bmatrix}, \; x(s,t) = \begin{bmatrix} x^h(s,t) \\ x^v(s,t) \end{bmatrix},$$

$x^h(s,t) \in \mathbb{R}^{n_{hx}}$ and $x^v(s,t) \in \mathbb{R}^{n_{vx}}$ represent the horizontal and the vertical states respectively; $u(s,t) \in \mathbb{R}^m$ represents the control input; $\omega(s,t) \in \mathbb{R}^{n_\omega}$ represents the external disturbance, which belongs to $l_2([0,\infty),[0,\infty))$; and $y(s,t) \in \mathbb{R}^{n_y}$ means the controlled output. $A(\rho_{s,t})$, $B(\rho_{s,t})$, $C(\rho_{s,t})$, and $D(\rho_{s,t})$ are known constant matrices, which are related to the Markov jump process $\rho_{s,t}$. The variable $\rho_{s,t}$ is generated from the set $\mathbb{S}_1 = \{1,2,\ldots,N_1\}$ with the transition probability matrix (TPM) $\Lambda = [\lambda_{pq}]_{N_1 \times N_1}$, which can be formulated as follows:

$$\lambda_{pq} = \Pr\{\rho_{s+1,t} = q | \rho_{s,t} = p\} = \Pr\{\rho_{s,t+1} = q | \rho_{s,t} = p\} \tag{2}$$

with

$$\begin{cases} \lambda_{pq} \in [0,1], \\ \sum_{q=1}^{N_1} \lambda_{pq} = 1. \end{cases} \tag{3}$$

The boundary condition (X_0, M_0) of 2-D MJS (1) is given as:

$$\begin{cases} X_0 = \{x^h(0,t), x^v(s,0) | s,t \in \mathcal{N}_+\}, \\ M_0 = \{\rho_{0,t}, \rho_{s,0} | s,t \in \mathcal{N}_+\}. \end{cases} \tag{4}$$

The zero boundary condition is assumed as $X_0 = \{0\}$. Furthermore, the following assumption is imposed on the boundary condition.

Assumption 1. *[21] Assume the boundary condition X_0 satisfies*

$$\lim_{T\to\infty} \mathbb{E}\left\{\sum_{t=0}^{T}(\|x^h(0,t)\|^2 + \|x^v(t,0)\|^2)\right\} < \infty.$$

B. Multiaccess stochastic communication protocol

As depicted in Fig. 1, 2-D MJS (1) has m actuators connected to the communication network. Due to network bandwidth and data rate limitations, only a portion of the signal can be transmitted between the actuator and controller.

In a multi-node control system, the C/A channel can accommodate $n(1 \le n \le m)$ actuator nodes to receive control signals at the same time. The access state of each actuator node is defined by the variable $\phi_\iota(s,t) : \mathbb{Z}^+ \to \{0,1\}$, which indicates whether the ι-th actuator can access the communication channel and receive the control signal at the time (s,t). The control signal is represented by

$$u(s,t) = \Phi_{\sigma_{s,t}} v(s,t)$$

with $\Phi_{\sigma_{s,t}} = \mathbf{diag}\{\phi_1(s,t), \phi_2(s,t), \ldots, \phi_m(s,t)\}$. $\sigma_{s,t} \in \mathbb{S}_2 \triangleq \{1,2,\ldots,N_2\}$ with $N_2 = C_m^n$ follows the conditional probability given by

$$\gamma_{\imath\jmath} = \Pr\{\sigma_{s+1,t} = \jmath | \sigma_{s,t} = \imath\} = \Pr\{\sigma_{s,t+1} = \jmath | \sigma_{s,t} = \imath\} \tag{5}$$

with $\gamma_{\imath\jmath} \in [0,1]$ and $\sum_{\jmath=1}^{N_2} \gamma_{\imath\jmath} = 1$. Define the TPM as $\Gamma = [\gamma_{\imath\jmath}]_{N_2 \times N_2}$.

Remark 1. *When only one actuator node is allowed to access the network at instant (s,t), i.e., $n = 1$, the proposed MSCP is simplified to the traditional stochastic communication protocol case, which has been extensively studied in [22–24]. Therefore, the stochastic communication protocol can be regarded as a particular instance of the MSCP. The MSCP, by better coordinating the scheduling and communication of multiple actuator nodes, reduces signal conflicts and resource waste, thereby optimizing the system's control performance, which will be shown in the subsequent simulation.*

The Markov chain in (2) is used to control the plant mode switch, and the Markov chain in (5) is used to manage access to actuator nodes. To simplify control design and stability analysis, we will introduce a new stochastic variable $\theta_{s,t}$ by using the mapping technique as in [25] to define a one-to-one mapping with Markov chains $\rho_{s,t}$ and $\sigma_{s,t}$

$$\theta_{s,t} = R(\rho_{s,t}, \sigma_{s,t}) = \rho_{s,t} + N_1(\sigma_{s,t} - 1) \tag{6}$$

with $\theta_{s,t} \in \mathbb{S} \triangleq \{1,\ldots,N\}$ and $N = N_1 \times N_2$.

Correspondingly, for a given $\theta_{s,t} \in \mathbb{S}$, the unique pair $(\rho_{s,t}, \sigma_{s,t})$ can be determined as follows:

$$\begin{cases} \rho_{s,t} \triangleq \eta_1(\theta_{s,t}) = \mathbf{mod}(\theta_{s,t} - 1, N_1) + 1, \\ \sigma_{s,t} \triangleq \eta_2(\theta_{s,t}) = \lfloor \dfrac{\theta_{s,t} - 1}{N_1} \rfloor + 1. \end{cases}$$

That is, the variable $\theta_{s,t}$ and the pair $(\rho_{s,t}, \sigma_{s,t})$ are one-to-one mapping.

At the same time, based on the transition probabilities (2) and (5), the conditional probability of the stochastic variable $\theta_{s,t}$ can be obtained as follows:

$$\begin{aligned} \pi_{ij} &= \Pr\{\theta_{s+1,t} = j | \theta_{s,t} = i\} = \Pr\{\theta_{s,t+1} = j | \theta_{s,t} = i\} \\ &= \Pr\{\rho_{s+1,t} = \eta_1(j), \sigma_{s+1,t} = \eta_2(j) | \rho_{s,t} = \eta_1(i), \\ &\quad \sigma_{s,t} = \eta_2(i)\} \\ &= \Pr\{\rho_{s,t+1} = \eta_1(j), \sigma_{s,t+1} = \eta_2(j) | \rho_{s,t} = \eta_1(i), \end{aligned}$$

$$\begin{aligned}&\sigma_{s,t}=\eta_2(i)\}\\&=\Pr\{\rho_{s+1,t}=\eta_1(j)|\rho_{s,t}=\eta_1(i)\}\\&\quad\times\Pr\{\sigma_{s+1,t}=\eta_2(j)|\sigma_{s,t}=\eta_2(i)\}\\&=\Pr\{\rho_{s,t+1}=\eta_1(j)|\rho_{s,t}=\eta_1(i)\}\\&\quad\times\Pr\{\sigma_{s,t+1}=\eta_2(j)|\sigma_{s,t}=\eta_2(i)\}\\&=\lambda_{\eta_1(i)\eta_1(j)}\gamma_{\eta_2(i)\eta_2(j)}.\end{aligned}\tag{7}$$

According to (7), the random variable $\theta_{s,t}$ follows the Markov chain, and its state transitions are described by TPM $\Pi=[\pi_{ij}]_{N\times N}$.

C. Controller model

To make the plant mode $\rho_{s,t}$ more accurately detected, the hidden Markov model (HMM) can be used, which is one of the popular models to describe the relationship between the detected mode and the plant mode [26, 27]. The detected mode is denoted by $\zeta_{s,t}$, which value varies in the finite set $\mathbb{S}_3=\{1,2,\ldots,N_3\}$; at the same time, it follows the conditional probability ψ_{pg} given $\rho_{s,t}$ as follows:

$$\Pr\{\zeta_{s,t}=g|\rho_{s,t}=p\}=\psi_{pg},$$

and $\Psi=\{\psi_{pg}\}$ signifies the conditional transition probability matrix (CTPM). For ψ_{pg}, the restrictions are similar to (3), i.e., $\psi_{pg}\in[0,1]$, $\sum_{g=1}^{N_3}\psi_{pg}=1$ for $\forall p\in\mathbb{S}_1$, $g\in\mathbb{S}_3$.

Combining the HMM and the MSCP, the following asynchronous state-feedback controller is proposed:

$$v(s,t)=K_{\zeta_{s,t}\sigma_{s,t}}x(s,t),\tag{8}$$

where $K_{\zeta_{s,t}\sigma_{s,t}}\in\mathbb{R}^{m\times(n_{hx}+n_{vx})}$ denotes the controller gain.

Remark 2. *The HMM used in this paper is a unified framework for asynchronous, synchronous, and mode-independent controllers. By adjusting the CTPM, the mode relationship between 2-D MJS (1) and its controller (8) can be flexibly controlled. Specifically, when the CTPM is set to the identity matrix, the controller mode $\zeta_{s,t}$ is completely consistent with the plant mode $\rho_{s,t}$, and the controller $v(s,t)=K_{\rho_{s,t}\sigma_{s,t}}x(s,t)$ performs synchronous control according to the actual state of the plant. When the CTPM has identical rows, the controller ignores the information of the plant mode $\rho_{s,t}$, and the controller becomes a mode-independent controller $v(s,t)=K_{\sigma_{s,t}}x(s,t)$.*

In the following, we will introduce some simple symbols to clarify and concise the expression. Specifically, the subscripts p, i, g, and $\imath$ will be used in place of the parameters $\rho_{s,t}$, $\theta_{s,t}$, $\zeta_{s,t}$, and $\sigma_{s,t}$, respectively. Then, the closed-loop 2-D MJS is obtained as follows:

$$\begin{cases}x^1(s,t)=(A_p+B_p\Phi_\imath K_{g\imath})x(s,t)+D_p\omega(s,t),\\y(s,t)=C_px(s,t).\end{cases}\tag{9}$$

Definition 1. *[28] Closed-loop 2-D MJS (9) with $\omega(s,t)=0$ is said to be SS if the following condition holds:*

$$\lim_{s+t\to\infty}\mathbb{E}\left\{\|x(s,t)\|^2\right\}=0\tag{10}$$

for any boundary condition (4).

Definition 2. *Assume that closed-loop 2-D MJS (9) satisfies (10). If there exist scalars $\mu>0$ and $\alpha\in[0,1]$ make the following condition holds:*

$$\begin{aligned}&\sum_{s=0}^{\infty}\sum_{t=0}^{\infty}\mathbb{E}\left\{(1-\alpha)y^T(s,t)y(s,t)-\mu^2\omega^T(s,t)\omega(s,t)\right\}\\&\qquad+\sup_{0\le s\le\infty}\sup_{0\le t\le\infty}\alpha y^T(s,t)y(s,t)<0,\end{aligned}\tag{11}$$

that is to say that the system satisfies $\mathcal{H}_\infty/\mathcal{L}_2-\mathcal{L}_\infty$ mixed performance.

Remark 3. *Note that Definition 2 can degenerate into a single performance index, $\mathcal{H}_\infty$ or $\mathcal{L}_2-\mathcal{L}_\infty$ performance index, by selecting different values of parameter α. Specifically, Definition 2 encompasses the two following cases.*

Case 1: When $\alpha=0$, Definition 2 degenerates into the $\mathcal{H}_\infty$ performance index, which reduces the impact of disturbance on system performance.

Case 2: When $\alpha=1$, Definition 2 degenerates into the $\mathcal{L}_2-\mathcal{L}_\infty$ performance, which adjusts the output of the systems to be minimum.

In this work, our goal is to develop a state-feedback controller subject to the MSCP to guarantee the closed-loop system is SS and satisfies $\mathcal{H}_\infty/\mathcal{L}_2-\mathcal{L}_\infty$ mixed performance.

III. Main Results

Next, we will provide sufficient conditions for closed-loop 2-D MJS (9) to ensure that the system is SS.

Lemma 1. *Under Assumption 1, closed-loop 2-D MJS (9) is SS, if there exist matrices $P_i=\mathbf{diag}\{P_i^h,P_i^v\}>0$, $R_{i\imath}>0$, and $K_{g\imath}$, for $i\in\mathbb{S}$, $\imath\in\mathbb{S}_2$, and $g\in\mathbb{S}_3$, such that the following conditions hold:*

$$\sum_{g=1}^{N_3}\psi_{pg}R_{i\imath}<P_i,\tag{12}$$

$$\begin{bmatrix}-\bar{P}_i^{-1}&A_p+B_p\Phi_\imath K_{g\imath}\\*&-R_{i\imath}\end{bmatrix}<0,\tag{13}$$

where $\bar{P}_i=\sum_{i=1}^{N}\pi_{ij}P_j$.

Proof: Choose a Lyapunov function given by

$$V(s,t)=x^T(s,t)P_ix(s,t),$$

here $P_i=\mathbf{diag}\{P^h_{\theta_{s,t}},P^v_{\theta_{s,t}}\}$. Let

$$\begin{aligned}\triangle V(s,t)=&x^{1T}(i,j)P_jx^1(s,t)-x^T(s,t)P_ix(s,t)\\=&x^T(s,t)(A_p+B_p\Phi_\imath K_{g\imath})^TP_j(A_p\\&+B_p\Phi_\imath K_{g\imath})x(s,t)-x^T(s,t)P_ix(s,t)\\&+\mathbf{He}\left(x^T(s,t)(A_p+B_p\Phi_\imath K_{g\imath})^TP_jD_p\omega(s,t)\right)\\&+\omega^T(s,t)D_p^TP_jD_p\omega(s,t),\end{aligned}\tag{14}$$

where $P_j=\mathbf{diag}\{P^h_{\theta_{s+1,t}},P^v_{\theta_{s,t+1}}\}$. Setting $\omega(s,t)=0$, and performing expectation operation for $\triangle V(s,t)$, one has

$$\begin{aligned}\mathbb{E}\{\triangle V(s,t)\}=\mathbb{E}\Big\{&x^T(s,t)\Big(\sum_{g=1}^{N_3}\psi_{pg}(A_p+B_p\Phi_\imath K_{g\imath})^T\\&\times\bar{P}_i(A_p+B_p\Phi_\imath K_{g\imath})\Big)x(s,t)\\&-x^T(s,t)P_ix(s,t)\Big\}.\end{aligned}\tag{15}$$

Using the Schur complement, (13) guarantees that

$$(A_p + B_p\Phi_\imath K_{g\imath})^T \bar{P}_i (A_p + B_p\Phi_\imath K_{g\imath}) < R_{ig}. \tag{16}$$

Then by (15) and (16), we obtain

$$\begin{aligned}\mathbb{E}\{\triangle V(s,t)\} &< \mathbb{E}\left\{x^T(s,t)\left(\sum_{g=1}^{N_3}\psi_{pg}R_{ig} - P_i\right)x(s,t)\right\} \\ &\leq -\beta_1 \mathbb{E}\left\{\|x(s,t)\|^2\right\},\end{aligned} \tag{17}$$

where β_1 denotes the minimum eigenvalue of $(P_i - \sum_{g=1}^{N_3}\psi_{pg}R_{ig})$. It follows from (12) that $\beta_1 > 0$. Adding both sides of (17) yields

$$\mathbb{E}\left\{\sum_{s=0}^{d_1}\sum_{t=0}^{d_2}\|x(s,t)\|^2\right\} \leq -\frac{1}{\beta_1}\mathbb{E}\left\{\sum_{s=0}^{d_1}\sum_{t=0}^{d_2}\triangle V(s,t)\right\}, \tag{18}$$

where d_1 and d_2 are arbitrary positive integers. By substituting $x^1(s,t)$ and $P_i = \mathbf{diag}\{P_i^h, P_i^v\}$ into $\triangle V(s,t)$, we have

$$\begin{aligned}&\sum_{s=0}^{d_1}\sum_{t=0}^{d_2}\triangle V(s,t) \\ &= \sum_{t=0}^{d_2}[x^{hT}(d_1+1,t)P^h_{\theta_{d_1+1,t}}x^h(d_1+1,t) \\ &\quad - x^{hT}(0,t)P^h_{\theta_{0,t}}x^h(0,t)] \\ &\quad + \sum_{s=0}^{d_1}[x^{vT}(s,d_2+1)P^v_{\theta_{s,d_2+1}}x^v(s,d_2+1) \\ &\quad - x^{vT}(s,0)P^v_{\theta_{s,0}}x^v(s,0)].\end{aligned} \tag{19}$$

It follows from (18) and (19) that

$$\begin{aligned}\mathbb{E}\left\{\sum_{s=0}^{d_1}\sum_{t=0}^{d_2}\|x(s,t)\|^2\right\} \leq &\frac{1}{\beta_1}\mathbb{E}\Big\{\sum_{t=0}^{d_2}x^{hT}(0,t)P^h_{\theta_{0,t}}x^h(0,t) \\ &+ \sum_{s=0}^{d_1}x^{vT}(s,0)P^v_{\theta_{s,0}}x^v(s,0)\Big\}.\end{aligned} \tag{20}$$

Let β_2 denote the maximum eigenvalue of $P^h_{\theta_{0,t}}$ and $P^v_{\theta_{s,0}}$, where $s,t = 0,1,2,\ldots$. If let d_1, d_2 tend to infinity in (20), then the following inequality holds:

$$\begin{aligned}&\mathbb{E}\left\{\sum_{s=0}^{d_1}\sum_{t=0}^{d_2}\|x(s,t)\|^2\right\} \\ &\leq \frac{\beta_2}{\beta_1}\mathbb{E}\Big\{\sum_{s=0}^{\infty}\|x^h(0,s)\|^2 + \|x^v(s,0)\|^2\Big\}.\end{aligned}$$

Recalling Assumption 1, it follows that:

$$\mathbb{E}\left\{\sum_{s=0}^{d_1}\sum_{t=0}^{d_2}\|x(s,t)\|^2\right\} < \infty,$$

which implies that closed-loop 2-D MJS (9) is SS. The proof has been ended. ■

In what follows, we analyze the stochastic stability and $\mathcal{H}_\infty/\mathcal{L}_2 - \mathcal{L}_\infty$ mixed performance of the closed-loop 2-D MJS (9).

Theorem 1. *Under Assumption 1, given the parameters $\mu > 0$, $0 \leq \alpha \leq 1$, closed-loop 2-D MJS (9) is SS and subject to $\mathcal{H}_\infty/\mathcal{L}_2 - \mathcal{L}_\infty$ mixed performance condition (11), if there exist matrices $P_i = \mathbf{diag}\{P_i^h, P_i^v\} > 0$, $R_{ig} > 0$, and $K_{g\imath}$, for $i \in \mathbb{S}$, $\imath \in \mathbb{S}_2$, and $g \in \mathbb{S}_3$, such that the following conditions hold:*

$$\sum_{g=1}^{N_3}\psi_{pg}R_{ig} < P_i, \tag{21}$$

$$\begin{bmatrix} -\bar{P}_i^{-1} & 0 & A_p + B_p\Phi_\imath K_{g\imath} & D_p \\ * & -I & \sqrt{1-\alpha}C_p & 0 \\ * & * & -R_{ig} & 0 \\ * & * & * & -\mu^2 I \end{bmatrix} < 0, \tag{22}$$

$$\begin{bmatrix} -I & \sqrt{\alpha}C_p \\ * & -P_i \end{bmatrix} < 0, \tag{23}$$

where $\bar{P}_i = \sum_{i=1}^{N}\pi_{ij}P_j$.

Proof: By employing the Schur complement, we can deduce (13) from (22). Following Lemma 1, it can be inferred that closed-loop 2-D MJS (9) is SS. Next, we only need to demonstrate that closed-loop 2-D MJS (9) satisfies $\mathcal{H}_\infty/\mathcal{L}_2 - \mathcal{L}_\infty$ mixed performance. To that purpose, we may introduce

$$\mathbf{J} = \sum_{s=0}^{\infty}\sum_{t=0}^{\infty}\mathbb{E}\left\{(1-\alpha)y^T(s,t)y(s,t) - \mu^2\omega^T(s,t)\omega(s,t)\right\}.$$

Under the zero boundary condition, we can obtain $\sum_{s=0}^{\infty}\sum_{t=0}^{\infty}\triangle V(s,t) \geq 0$ from (19). Based on (14) yields

$$\begin{aligned}\mathbf{J} &\leq \sum_{s=0}^{\infty}\sum_{t=0}^{\infty}\mathbb{E}\Big\{(1-\alpha)y^T(s,t)y(s,t) - \mu^2\omega^T(s,t)\omega(s,t) \\ &\qquad + \triangle V(s,t)\Big\} \\ &= \sum_{s=0}^{\infty}\sum_{t=0}^{\infty}\mathbb{E}\Big\{\hat{x}^T(s,t)\Big(\sum_{g=1}^{N_3}\psi_{pg}\hat{A}^T\hat{P}\hat{A} \\ &\qquad + \mathbf{diag}\left\{-P_i, -\mu^2 I\right\}\Big)\hat{x}(s,t)\Big\},\end{aligned} \tag{24}$$

where $\hat{x}(s,t) = \begin{bmatrix}x(s,t)\\ \omega(s,t)\end{bmatrix}$, $\hat{A} = \begin{bmatrix}A_p + B_p\Phi_\imath K_{g\imath}\\ \sqrt{1-\alpha}C_p\end{bmatrix}$, $\hat{P} = \mathbf{diag}\{\bar{P}_i, I\}$.

Noting (21), we can get from (24) that

$$\begin{aligned}\mathbf{J} \leq \sum_{s=0}^{\infty}\sum_{t=0}^{\infty}\mathbb{E}\Big\{\hat{x}^T(s,t)\Big(&\sum_{g=1}^{N_3}\psi_{pg}\hat{A}^T\hat{P}\hat{A} \\ &+ \mathbf{diag}\left\{-R_{ig}, -\mu^2 I\right\}\Big)\hat{x}(s,t)\Big\}.\end{aligned} \tag{25}$$

Considering (22) and (25), we can conclude that $\mathbf{J} < 0$, which means

$$\begin{aligned}\sum_{s=0}^{\infty}\sum_{t=0}^{\infty}\mathbb{E}\Big\{&(1-\alpha)y^T(s,t)y(s,t) - \mu^2\omega^T(s,t)\omega(s,t) \\ &+ \triangle V(s,t)\Big\} < 0.\end{aligned}$$

This implies that

$$\begin{aligned}&\sum_{s=0}^{\infty}\sum_{t=0}^{\infty}\mathbb{E}\left\{(1-\alpha)y^T(s,t)y(s,t) - \mu^2\omega^T(s,t)\omega(s,t)\right\} \\ &< -V(s,t).\end{aligned}$$

Therefore, we will calculate the following formula:

$$\sup_{0\leq s\leq\infty}\sup_{0\leq t\leq\infty}\alpha y^T(s,t)y(s,t) - V(s,t)$$

$$\leq \alpha x^T(s,t)(C_p^T C_p - P_i)x(s,t).$$

According to condition (23), the following inequality is derived:

$$\sup_{0\leq s\leq\infty}\sup_{0\leq t\leq\infty} \alpha y^T(s,t)y(s,t) - V(s,t) < 0.$$

With the help of the above proof process, it is evident that the following formula holds:

$$\sum_{s=0}^{\infty}\sum_{t=0}^{\infty}\mathbb{E}\left\{(1-\alpha)y^T(s,t)y(s,t) - \mu^2\omega^T(s,t)\omega(s,t)\right\} + \sup_{0\leq s\leq\infty}\sup_{0\leq t\leq\infty}\alpha y^T(s,t)y(s,t) < 0.$$

Based on the discussions mentioned above, it becomes evident that condition (11) in Definition 2 is satisfied. Thus, we can say that closed-loop 2-D MJS (9) satisfies $\mathcal{H}_\infty/\mathcal{L}_2 - \mathcal{L}_\infty$ mixed performance. With this, the proof is concluded. ■

Although Theorem 1 provides concise constraints to ensure closed-loop 2-D MJS (9) is SS and equips $\mathcal{H}_\infty/\mathcal{L}_2 - \mathcal{L}_\infty$ mixed performance condition (11), it is still difficult to directly use it for the controller design due to the presence of nonlinearity. As a result, we will eliminate the nonlinearity in Theorem 1 and develop LMI-based conditions.

Theorem 2. *Under Assumption 1, given the parameters $\tilde{\mu} > 0$, $0 \leq \alpha \leq 1$, if there exist matrices $\tilde{P}_i = \mathbf{diag}\{\tilde{P}_i^h, \tilde{P}_i^v\} > 0$, $\tilde{R}_{ig} > 0$, $M_{g\imath}$, and $\tilde{K}_{g\imath}$, for $i \in \mathbb{S}$, $\imath \in \mathbb{S}_2$, and $g \in \mathbb{S}_3$, such that the following conditions hold:*

$$\begin{bmatrix} -\tilde{P}_i & T_i \\ * & -\mathscr{R}_i \end{bmatrix} < 0, \tag{26}$$

$$\begin{bmatrix} -\mathscr{P} & 0 & \mathscr{A} & \mathscr{D} \\ * & -I & \sqrt{1-\alpha}C_p M_{g\imath} & 0 \\ * & * & \tilde{R}_{ig} - \mathbf{He}(M_{g\imath}) & 0 \\ * & * & * & -\tilde{\mu}I \end{bmatrix} < 0, \tag{27}$$

$$\begin{bmatrix} -I & \sqrt{\alpha}C_p\tilde{P}_i \\ * & -\tilde{P}_i \end{bmatrix} < 0, \tag{28}$$

where

$$\begin{aligned} T_i &= \left[\sqrt{\psi_{p1}}\tilde{P}_i \quad \sqrt{\psi_{p2}}\tilde{P}_i \quad \cdots \quad \sqrt{\psi_{pN_3}}\tilde{P}_i\right], \\ \mathscr{R}_i &= \mathbf{diag}\{\tilde{R}_{i1}, \tilde{R}_{i2}, \ldots, \tilde{R}_{iN_3}\}, \\ \mathscr{P} &= \mathbf{diag}\{\tilde{P}_1, \tilde{P}_2, \ldots, \tilde{P}_N\}, \\ \mathscr{A} &= \left[\sqrt{\pi_{i1}}U_A^T \quad \sqrt{\pi_{i2}}U_A^T \quad \cdots \quad \sqrt{\pi_{iN}}U_A^T\right]^T, \\ U_A &= A_p M_{g\imath} + B_p\Phi_\imath\tilde{K}_{g\imath}, \\ \mathscr{D} &= \left[\sqrt{\pi_{i1}}D_p^T \quad \sqrt{\pi_{i2}}D_p^T \quad \cdots \quad \sqrt{\pi_{iN}}D_p^T\right]^T, \end{aligned}$$

closed-loop 2-D MJS (9) is SS and satisfies $\mathcal{H}_\infty/\mathcal{L}_2 - \mathcal{L}_\infty$ mixed performance index $\mu = \sqrt{\tilde{\mu}}$. Furthermore, if feasible solutions exist for (26) - (28), the designed controller gain $K_{g\imath}$ can be obtained by

$$K_{g\imath} = \tilde{K}_{g\imath}M_{g\imath}^{-1}.$$

Proof: In Theorem 2, the coupling terms in Theorem 1 are successfully handled by introducing a slack matrix $M_{g\imath}$. It can be deduced from (27) that $\tilde{R}_{ig} - \mathbf{He}(M_{g\imath}) < 0$, that is, $\mathbf{He}(M_{g\imath})$ is positive definite. This indicates that the matrix $M_{g\imath}$ should be invertible. Here, some notations are defined by

$$\tilde{P}_i = P_i^{-1},\ \tilde{R}_{ig} = R_{ig}^{-1},\ \tilde{K}_{g\imath} = K_{g\imath}M_{g\imath},\ \tilde{\mu} = \mu^2.$$

We will prove through the Schur complement that (21) and (26) are equivalent. For this purpose, we establish the equivalence between (21) and the following inequality:

$$\begin{bmatrix} -P_i & \bar{T}_i \\ * & -\mathscr{R}_i \end{bmatrix} < 0, \tag{29}$$

where $\bar{T}_i = \left[\sqrt{\psi_{p1}}I \quad \sqrt{\psi_{p2}}I \quad \cdots \quad \sqrt{\psi_{pN_3}}I\right]$. Then, we can pre-multiply and post-multiply (29) with $\mathbf{diag}\{\tilde{P}_i, I\}$ to obtain (26).

Subsequently, we will verify (27) to ensure that (22) is established. It is easy to find that

$$(M_{g\imath} - \tilde{R}_{ig})^T\tilde{R}_{ig}^{-1}(M_{g\imath} - \tilde{R}_{ig}) \geq 0,$$

which can be rewritten as

$$-M_{g\imath}^T\tilde{R}_{ig}^{-1}M_{g\imath}^T \leq \tilde{R}_{ig} - \mathbf{He}(M_{g\imath}). \tag{30}$$

Thanks to (27) and (30), the following condition holds:

$$\begin{bmatrix} -\mathscr{P} & 0 & \mathscr{A} & \mathscr{D} \\ * & -I & \sqrt{1-\alpha}C_p M_{g\imath} & 0 \\ * & * & -M_{g\imath}^T\tilde{R}_{ig}^{-1}M_{g\imath}^T & 0 \\ * & * & * & -\tilde{\mu}I \end{bmatrix} < 0. \tag{31}$$

Using $\mathbf{diag}\{I, I, (M_{g\imath}^T)^{-1}, I\}$ and its transpose to pre-multiply and post-multiply (31), respectively, we obtain

$$\begin{bmatrix} -\mathscr{P} & 0 & \bar{\mathscr{A}} & \mathscr{D} \\ * & -I & \sqrt{1-\alpha}C_p & 0 \\ * & * & -R_{ig} & 0 \\ * & * & * & -\tilde{\mu}I \end{bmatrix} < 0,$$

where $\bar{\mathscr{A}} = \left[\sqrt{\pi_{i1}}\bar{U}_A^T \quad \sqrt{\pi_{i2}}\bar{U}_A^T \quad \cdots \quad \sqrt{\pi_{iN}}\bar{U}_A^T\right]^T$ and $\bar{U}_A = A_p + B_p\Phi_\imath K_{g\imath}$. By successively applying the Schur complement, (22) can be obtained. Then, pre- and post-multiplying (28) by $\mathbf{diag}\{I, P_i^{-1}\}$, and employing the Schur complement again, we can obtain (23). This completes the proof. ■

Remark 4. *Theorem 2 transforms the controller design problem into a linear matrix inequality (LMI) based problem by eliminating nonlinearities, which can be efficiently solved using the MOSEK optimization toolbox for MATLAB. The optimal $\mathcal{H}_\infty/\mathcal{L}_2 - \mathcal{L}_\infty$ mixed performance is obtained by solving the following convex optimization issue:*

$$\begin{aligned} &\textit{min } \mu \\ &\textit{s.t. LMIs } (26),\ (27),\ \textit{and } (28). \end{aligned}$$

If the number of actuator nodes accessing the network is fixed to one, the MSCP will degenerate into the traditional stochastic communication protocol. Then, we can obtain the following result:

Corollary 1. *Under Assumption 1, given the parameters $\tilde{\mu} > 0$, $0 \leq \alpha \leq 1$, if there exist matrices $\tilde{P}_i = \mathbf{diag}\{\tilde{P}_i^h, \tilde{P}_i^v\} > 0$, $\tilde{R}_{ig} > 0$, $M_{g\imath}$, and $\tilde{K}_{g\imath}$, for $i \in \mathbb{S}$, $g \in \mathbb{S}_3$, and $\imath \in \mathbb{S}_4$, such that the following conditions hold:*

$$\begin{bmatrix} -\tilde{P}_i & T_i \\ * & -\mathscr{R}_i \end{bmatrix} < 0, \tag{32}$$

$$\begin{bmatrix} -\mathscr{P} & 0 & \mathscr{A} & \mathscr{D} \\ * & -I & \sqrt{1-\alpha}C_p M_{g\imath} & 0 \\ * & * & \tilde{R}_{ig} - \mathbf{He}(M_{g\imath}) & 0 \\ * & * & * & -\tilde{\mu}I \end{bmatrix} < 0, \tag{33}$$

$$\begin{bmatrix} -I & \sqrt{\alpha}C_p\tilde{P}_i \\ * & -\tilde{P}_i \end{bmatrix} < 0, \tag{34}$$

where

$$\begin{aligned} T_i &= \left[\sqrt{\psi_{p1}}\tilde{P}_i \quad \sqrt{\psi_{p2}}\tilde{P}_i \quad \cdots \quad \sqrt{\psi_{pN_3}}\tilde{P}_i\right], \\ \mathscr{R}_i &= \mathbf{diag}\{\tilde{R}_{i1}, \tilde{R}_{i2}, \ldots, \tilde{R}_{iN_3}\}, \\ \mathscr{P} &= \mathbf{diag}\{\tilde{P}_1, \tilde{P}_2, \ldots, \tilde{P}_N\}, \\ \mathscr{A} &= \left[\sqrt{\pi_{i1}}U_A^T \quad \sqrt{\pi_{i2}}U_A^T \quad \cdots \quad \sqrt{\pi_{iN}}U_A^T\right]^T, \\ U_A &= A_pM_{g\imath} + B_pI_\imath\tilde{K}_{g\imath}, \\ \mathscr{D} &= \left[\sqrt{\pi_{i1}}D_p^T \quad \sqrt{\pi_{i2}}D_p^T \quad \cdots \quad \sqrt{\pi_{iN}}D_p^T\right]^T, \\ I_\imath &= \mathbf{diag}\{\underbrace{0, ..., 0}_{\imath-1}, 1, \underbrace{0, ..., 0}_{m-\imath}\}, \end{aligned}$$

closed-loop 2-D MJS (9) is SS and satisfies $\mathcal{H}_\infty/\mathcal{L}_2 - \mathcal{L}_\infty$ mixed performance index $\mu = \sqrt{\tilde{\mu}}$. Furthermore, if feasible solutions exist for (32) - (34), the designed controller gain $K_{g\imath}$ can be obtained by

$$K_{g\imath} = \tilde{K}_{g\imath}M_{g\imath}^{-1}.$$

Considering the case where there is no stochastic communication protocol, the following corollary can be drawn:

Corollary 2. *Under Assumption 1, given the parameters $\tilde{\mu} > 0$, $0 \le \alpha \le 1$, if there exist matrices $\tilde{P}_p = \mathbf{diag}\{\tilde{P}_p^h, \tilde{P}_p^v\} > 0$, $\tilde{R}_{pg} > 0$, M_g, and $\tilde{K}_g$, for $g \in \mathbb{S}_3$ and $p \in \mathbb{S}_5$, such that the following conditions hold:*

$$\begin{bmatrix} -\tilde{P}_p & T_p \\ * & -\mathscr{R}_p \end{bmatrix} < 0, \tag{35}$$

$$\begin{bmatrix} -\mathscr{P} & 0 & \mathscr{A} & \mathscr{D} \\ * & -I & \sqrt{1-\alpha}C_pM_g & 0 \\ * & * & \tilde{R}_{pg} - \mathbf{He}(M_g) & 0 \\ * & * & * & -\tilde{\mu}I \end{bmatrix} < 0, \tag{36}$$

$$\begin{bmatrix} -I & \sqrt{\alpha}C_p\tilde{P}_p \\ * & -\tilde{P}_p \end{bmatrix} < 0, \tag{37}$$

where

$$\begin{aligned} T_p &= \left[\sqrt{\psi_{p1}}\tilde{P}_p \quad \sqrt{\psi_{p2}}\tilde{P}_p \quad \cdots \quad \sqrt{\psi_{pN_3}}\tilde{P}_p\right], \\ \mathscr{R}_p &= \mathbf{diag}\{\tilde{R}_{p1}, \tilde{R}_{p2}, \ldots, \tilde{R}_{pN_3}\}, \\ \mathscr{P} &= \mathbf{diag}\{\tilde{P}_1, \tilde{P}_2, \ldots, \tilde{P}_{N_1}\}, \\ \mathscr{A} &= \left[\sqrt{\pi_{i1}}U_A^T \quad \sqrt{\pi_{i2}}U_A^T \quad \cdots \quad \sqrt{\pi_{iN_1}}U_A^T\right]^T, \\ U_A &= A_pM_g + B_p\tilde{K}_g, \\ \mathscr{D} &= \left[\sqrt{\pi_{i1}}D_p^T \quad \sqrt{\pi_{i2}}D_p^T \quad \cdots \quad \sqrt{\pi_{iN_1}}D_p^T\right]^T, \end{aligned}$$

closed-loop 2-D MJS (9) is SS and satisfies $\mathcal{H}_\infty/\mathcal{L}_2 - \mathcal{L}_\infty$ mixed performance index $\mu = \sqrt{\tilde{\mu}}$. Furthermore, if feasible solutions exist for (35) - (37), the designed controller gain $K_{g\imath}$ can be obtained by

$$K_g = \tilde{K}_gM_g^{-1}.$$

IV. Numerical Example

In practical engineering, the Darboux equation [29] can effectively describe various dynamic processes, such as infectious prediction [30], fluid motion [31], and investment securities [32]. This paper assumes that the parameters of the Darboux equation obey the Markov random process. Using the same modeling technology as [33], a 2-D difference model in the form of 2-D MJS (1) is generated with

Mode 1:

$$A_1 = \begin{bmatrix} -0.9 & 0.5 \\ -0.2 & -1.5 \end{bmatrix}, B_1 = \begin{bmatrix} -0.2 & 0.3 & 0.3 \\ -0.2 & 0.5 & 0.45 \end{bmatrix},$$
$$D_1 = \begin{bmatrix} 0.1 \\ 0.2 \end{bmatrix}, C_1 = \begin{bmatrix} 1 & 0 \\ 1 & 0.6 \end{bmatrix}.$$

Mode 2:

$$A_2 = \begin{bmatrix} -1.1 & 0.6 \\ -0.3 & -2.2 \end{bmatrix}, B_2 = \begin{bmatrix} 0.2 & 0.3 & 0.3 \\ -0.3 & 0.4 & 0.55 \end{bmatrix},$$
$$D_2 = \begin{bmatrix} 0.2 \\ 0.1 \end{bmatrix}, C_2 = \begin{bmatrix} 1 & 0 \\ 1 & 0.6 \end{bmatrix}.$$

The jump of the plant is assumed to adhere to the TPM Λ as follows:

$$\Lambda = \begin{bmatrix} 0.6 & 0.4 \\ 0.5 & 0.5 \end{bmatrix}.$$

In the C/A channel, three possible transmission combinations are formed by randomly selecting two actuator nodes for transmission at each moment, i.e., $\Phi_1 = \mathbf{diag}\{1, 1, 0\}, \Phi_2 = \mathbf{diag}\{0, 1, 1\}, \Phi_3 = \mathbf{diag}\{1, 0, 1\}$. Assume that the TPM Γ is given as

$$\Gamma = \begin{bmatrix} 0.4 & 0.4 & 0.2 \\ 0.3 & 0.3 & 0.4 \\ 0.2 & 0.2 & 0.6 \end{bmatrix}.$$

According to the mapping relationship in (6), the relation between the pair $(\rho_{s,t}, \sigma_{s,t})$ and the variable $\theta_{s,t}$ is provided in TABLE I. In addition, based on (7), the TPM for the new random variable $\theta_{s,t}$ can be obtained as follows:

$$\Pi = \begin{bmatrix} 0.24 & 0.16 & 0.24 & 0.16 & 0.12 & 0.08 \\ 0.20 & 0.20 & 0.20 & 0.20 & 0.10 & 0.10 \\ 0.18 & 0.12 & 0.18 & 0.12 & 0.24 & 0.16 \\ 0.15 & 0.15 & 0.15 & 0.15 & 0.20 & 0.20 \\ 0.12 & 0.08 & 0.12 & 0.08 & 0.36 & 0.24 \\ 0.10 & 0.10 & 0.10 & 0.10 & 0.30 & 0.30 \end{bmatrix}.$$

Then, assume that the CTPMs Ψ are as follows:

$$\Psi_1 = \begin{bmatrix} 0.1 & 0.9 \\ 0.8 & 0.2 \end{bmatrix}, \Psi_2 = \begin{bmatrix} 1 & 0 \\ 0 & 1 \end{bmatrix}, \Psi_3 = \begin{bmatrix} 0 & 1 \\ 0 & 1 \end{bmatrix},$$

indicating the asynchronous, synchronous, and mode-independent case of closed-loop 2-D MJS (9) and its controller, respectively. For different values of the scalar α and

TABLE I
Relation of $(\rho_{s,t}, \sigma_{s,t})$ and $\theta_{s,t}$

$(\rho_{s,t}, \sigma_{s,t})$	$\theta_{s,t}$	$(\rho_{s,t}, \sigma_{s,t})$	$\theta_{s,t}$
(1, 1)	1	(2, 1)	2
(1, 2)	3	(2, 2)	4
(1, 3)	5	(2, 3)	6

TABLE II
Optimal μ for different α and CTPM.

α	μ		
	Ψ_1	Ψ_2	Ψ_3
0.6	1.2075	0.7127	1.5094
0.7	1.0457	0.6663	1.3072
0.8	0.8864	0.6380	1.0679

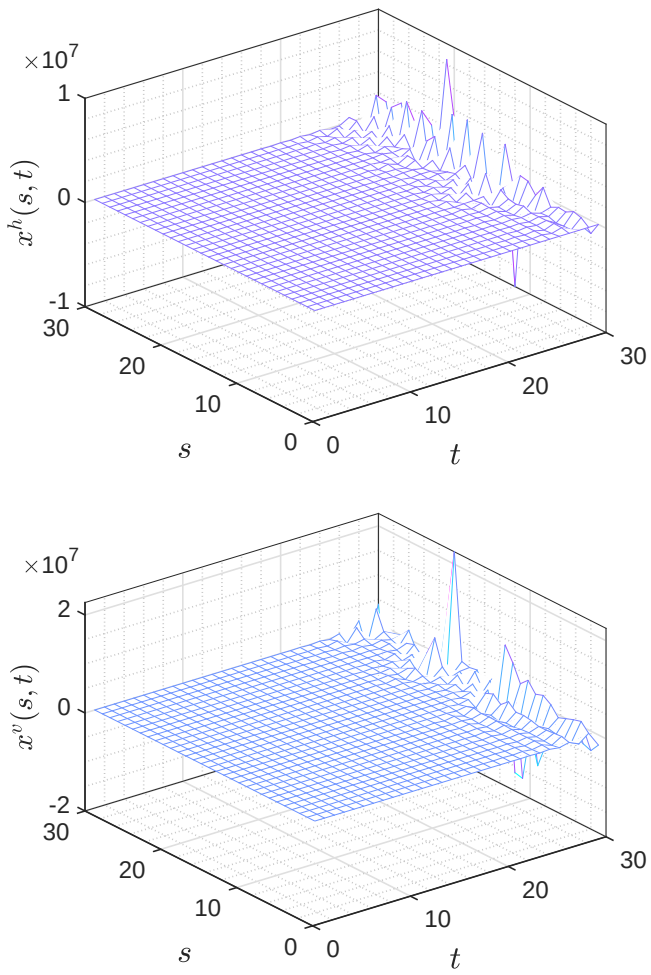

Fig. 2. State trajectories $x^h(s,t)$ and $x^v(s,t)$ in the open-loop case

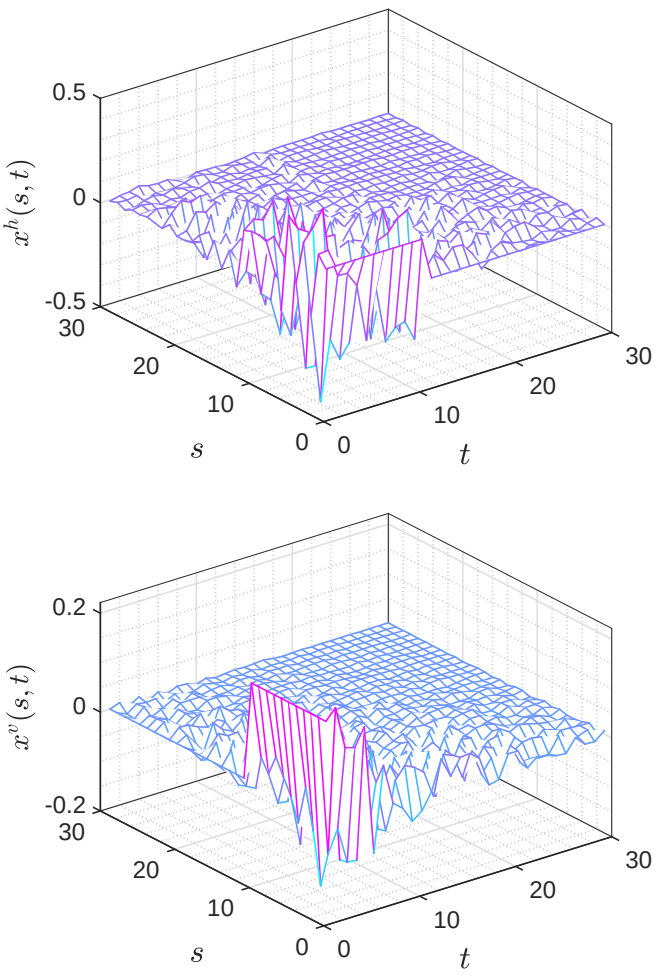

Fig. 3. State trajectories $x^h(s,t)$ and $x^v(s,t)$ in the closed-loop case

the CTPMs, TABLE II lists the optimal value μ regarding $\mathcal{H}_\infty/\mathcal{L}_2-\mathcal{L}_\infty$ mixed performance based on Theorem 2. It is evident that in each CTPM case, μ decreases as α increases, indicating that a higher α results in improved $\mathcal{H}_\infty/\mathcal{L}_2-\mathcal{L}_\infty$ mixed performance of closed-loop 2-D MJS (9).

By solving Theorem 2 with $\alpha = 0.6$, we can obtain the state-feedback controller gains as

$$K_{11}=\begin{bmatrix}0.9730 & -3.8035\\ 1.1371 & 1.8772\\ 0 & 0\end{bmatrix}, K_{21}=\begin{bmatrix}0.1559 & -0.8422\\ 0.6966 & 3.0250\\ 0 & 0\end{bmatrix},$$
$$K_{12}=\begin{bmatrix}0 & 0\\ 0.1372 & -2.1678\\ 0.5716 & 5.3295\end{bmatrix}, K_{22}=\begin{bmatrix}0 & 0\\ -0.3883 & -1.3569\\ 0.9969 & 4.6200\end{bmatrix},$$
$$K_{13}=\begin{bmatrix}2.0105 & -2.8528\\ 0 & 0\\ 1.5213 & 2.0187\end{bmatrix}, K_{23}=\begin{bmatrix}0.4816 & -0.4244\\ 0 & 0\\ 0.8035 & 3.0920\end{bmatrix},$$

with the $\mathcal{H}_\infty/\mathcal{L}_2-\mathcal{L}_\infty$ mixed performance index $\mu = 1.2075$.

If we assume that the network channels permit only one actuator node to transmit signals at each time, in this case, the MSCP proposed in this paper will be simplified to the stochastic communication protocol. By solving Corollary 1 with $\alpha = 0.6$, we can obtain the state-feedback controller gains as

$$K_{11}=\begin{bmatrix}-0.9439 & -6.4214\\ 0 & 0\\ 0 & 0\end{bmatrix}, K_{21}=\begin{bmatrix}-0.9894 & -6.4621\\ 0 & 0\\ 0 & 0\end{bmatrix},$$
$$K_{12}=\begin{bmatrix}0 & 0\\ 0.6478 & 2.7964\\ 0 & 0\end{bmatrix}, K_{22}=\begin{bmatrix}0 & 0\\ 0.5488 & 3.9078\\ 0 & 0\end{bmatrix},$$
$$K_{13}=\begin{bmatrix}0 & 0\\ 0 & 0\\ 0.5633 & 3.4714\end{bmatrix}, K_{23}=\begin{bmatrix}0 & 0\\ 0 & 0\\ 0.5274 & 3.6091\end{bmatrix},$$

with $\mathcal{H}_\infty/\mathcal{L}_2-\mathcal{L}_\infty$ mixed performance index $\mu = 8.2116$. Through more effective actuator node scheduling, the MSCP-proposed control scheme can greatly enhance control performance, according to a comparison of the outcomes of the two scenarios.

Next, we'll demonstrate the effectiveness by comparing the evolutions of system states with and without control input. As a result, it is necessary to present the boundary condition and disturbance input. In addition, set the disturbance as $\omega(s,t) = 0.9^{s+t}\omega^*(s,t)$, where $\omega^*(s,t)$ takes values in -1 or 1, and specify the initial states given by

$$x^h(0,t)=\begin{cases}0.2, & t=0,1,\ldots,10;\\ 0, & \text{elsewhere.}\end{cases}$$

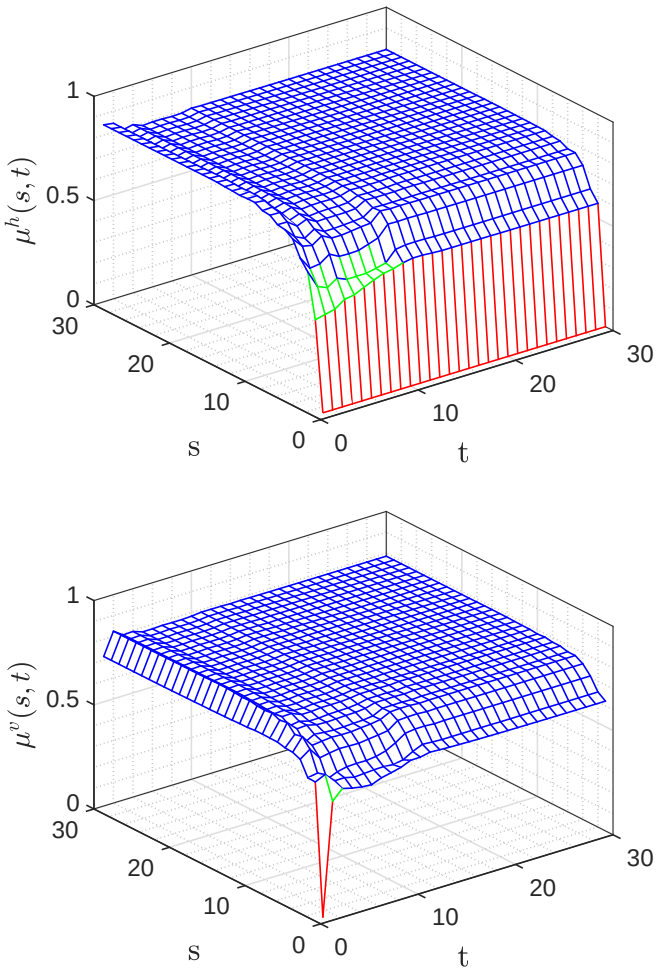

Fig. 4. Horizontal and vertical trajectories of two binary functions

$$x^v(s,0) = \begin{cases} 0.2, & s = 0, 1, \ldots, 10; \\ 0, & \text{elsewhere.} \end{cases}$$

In this way, the state trajectories of uncontrolled 2-D MJS (1) are shown in Fig. 2. It can be seen in the figure that the horizontal and vertical states show a trend toward infinity, which indicates that the system is unstable. However, by using the controller based on Theorem 2, the state trajectories of closed-loop 2-D MJS (9) in both directions are shown in Fig. 3, which shows that the controller designed in Theorem 2 is effective.

To measure $\mathcal{H}_\infty/\mathcal{L}_2 - \mathcal{L}_\infty$ mixed performance of closed-loop 2-D MJS (9), according to Definition 2, we introduce the following two binary functions:

$$\mu^h(s,t) = \frac{\sqrt{(1-\alpha)\sum_{s=0}^{\infty}\sum_{t=0}^{\infty}\|y^h(s,t)\|^2}}{\|\omega(s,t)\|_2} + \frac{\sqrt{\alpha \sup_{0\le s\le\infty}\sup_{0\le t\le\infty}\|y^h(s,t)\|^2}}{\|\omega(s,t)\|_2},$$

$$\mu^v(s,t) = \frac{\sqrt{(1-\alpha)\sum_{s=0}^{\infty}\sum_{t=0}^{\infty}\|y^v(s,t)\|^2}}{\|\omega(s,t)\|_2} + \frac{\sqrt{\alpha \sup_{0\le s\le\infty}\sup_{0\le t\le\infty}\|y^v(s,t)\|^2}}{\|\omega(s,t)\|_2}.$$

Fig. 4 depicts the trajectories of $\mu^h(s,t)$ and $\mu^v(s,t)$. The trajectories of $\mu^h(s,t)$ and $\mu^v(s,t)$ obtained by the proposed method finally converge to 0.7821 and 0.7659, respectively, both less than the minimum value $\mu = 1.2075$. The above results show the effectiveness of the state-feedback controller design method proposed in this paper.

TABLE III
COMPARISONS OF μ FOR DIFFERENT METHODS.

Methods	μ		
	Ψ_1	Ψ_2	Ψ_3
Theorem 2 in [6]	1.2331	0.6848	1.5245
Corollary 2	0.7799	0.4627	0.9642

Finally, we investigate the case without the stochastic communication protocol, in which both Corollary 2 and Theorem 2 in [6] apply. Table III provides the optimal performance index μ for different CTPM selections based on the LMIs in Corollary 2 and Theorem 2 in [6]. It can be observed that the optimal value of μ obtained by the method in [6] is consistently higher than the optimal value obtained by Corollary 2. Therefore, under the same parameter conditions, our proposed method is less conservative than the method given in [6].

V. CONCLUSIONS

In this paper, we have devoted ourselves to investigating the $\mathcal{H}_\infty/\mathcal{L}_2 - \mathcal{L}_\infty$ mixed control problem of 2-D MJS (9), where the MSCP has been adopted to schedule transmission nodes. A new Markov chain (7) has been introduced to simultaneously characterize plant mode switch and actuator access states. Then, using Lyapunov's direct method, a sufficient condition has been obtained to ensure that closed-loop 2-D MJS is SS and satisfies $\mathcal{H}_\infty/\mathcal{L}_2 - \mathcal{L}_\infty$ mixed performance. Furthermore, the state-feedback controller has been designed through an optimization technique. Finally, the feasibility and applicability of our proposed state-feedback controller have been verified through an example related to the Darboux equation.

REFERENCES

[1] D. Bors and S. Walczak, "Application of 2D systems to investigation of a process of gas filtration," *Multidimensional Systems and Signal Processing*, vol. 23, no. 1-2, pp. 119–130, 2012.

[2] W. Paszke, R. Merry, and R. van de Molengraft, "Iterative learning control by two-dimensional system theory applied to a motion system," in *American Control Conference, New York, USA*. IEEE, 2007, pp. 5484–5489.

[3] M. Li and D. Wang, "2-D stochastic configuration networks for image data analytics," *IEEE Transactions on Cybernetics*, vol. 51, no. 1, pp. 359–372, 2021.

[4] C. K. Ahn, P. Shi, and M. V. Basin, "Two-dimensional dissipative control and filtering for Roesser model," *IEEE Transactions on Automatic Control*, vol. 60, no. 7, pp. 1745–1759, 2015.

[5] T. Hinamoto, "Stability of 2-D discrete systems described by the Fornasini-Marchesini second model," *IEEE Transactions on Circuits and Systems I: Fundamental Theory and Applications*, vol. 44, no. 3, pp. 254–257, 1997.

[6] Z. Wu, Y. Shen, P. Shi, Z. Shu, and H. Su, "$\mathcal{H}_\infty$ control for 2-D Markov jump systems in Roesser model," *IEEE Transactions on Automatic Control*, vol. 64, no. 1, pp. 427–432, 2019.

[7] I. Ghous, Z. Xiang, and H. R. Karimi, "$\mathcal{H}_\infty$ control of 2-D continuous Markovian jump delayed systems with partially unknown transition probabilities," *Information Sciences*, vol. 382, pp. 274–291, 2017.

[8] J. Zhu, C. Li, and G. E. Dullerud, "Asynchronous $\mathcal{H}_\infty$ control for two-dimensional hidden Markovian jump systems with partly known mode observation conditional probabilities," *International Journal of Robust and Nonlinear Control*, vol. 30, no. 8, pp. 3344–3364, 2020.

[9] Y. Pan, Q. Li, H. Liang, and H.-K. Lam, "A novel mixed control approach for fuzzy systems via membership functions online learning policy," *IEEE Transactions on Fuzzy Systems*, vol. 30, no. 9, pp. 3812–3822, 2022.

[10] J. Li, Y. Niu, and Y. Yang, "Output-feedback control under hidden Markov analog fading and redundant channels," *IEEE Transactions on Circuits and Systems II: Express Briefs*, vol. 68, no. 8, pp. 2922–2926, 2021.

[11] B. Zheng and G. Yang, "$\mathcal{H}_2$ control of linear uncertain systems considering input quantization with encoder/decoder mismatch," *ISA Transactions*, vol. 52, no. 5, pp. 577–582, 2013.

[12] J. Wang, Y. Song, G. Wei, and Y. Dong, "Robust model predictive control for polytopic uncertain systems with state saturation nonlinearities under round-robin protocol," *International Journal of Robust and Nonlinear Control*, vol. 29, no. 7, pp. 2188–2202, 2019.

[13] L. Zou, Z. Wang, Q. Han, and D. Zhou, "Ultimate boundedness control for networked systems with try-once-discard protocol and uniform quantization effects," *IEEE Transactions on Automatic Control*, vol. 62, no. 12, pp. 6582–6588, 2017.

[14] J. Song, Z. Wang, Y. Niu, and J. Hu, "Observer-based sliding mode control for state-saturated systems under weighted try-once-discard protocol," *International Journal of Robust and Nonlinear Control*, vol. 30, no. 18, pp. 7991–8006, 2020.

[15] X. Lv, Y. Niu, and J. Song, "Sliding mode control for uncertain 2D systems under stochastic communication protocol: The Roesser model case," *IEEE Transactions on Circuits and Systems II: Express Briefs*, vol. 69, no. 3, pp. 1228–1232, 2022.

[16] Y. Zhang, Y. Ji, T. Jiang, and J. Zhou, "Event-triggered control for Roesser model-based 2D Markov jump systems under stochastic communication protocol," *Circuits, Systems, and Signal Processing*, pp. 1–24, 2024.

[17] M. Donkers, W. Heemels, D. Bernardini, A. Bemporad, and V. Shneer, "Stability analysis of stochastic networked control systems," *Automatica*, vol. 48, no. 5, pp. 917–925, 2012.

[18] W. Chen, J. Hu, Z. Wu, X. Yi, and H. Liu, "Protocol-based fault detection for state-saturated systems with sensor nonlinearities and redundant channels," *Applied Mathematics and Computation*, vol. 475, p. 128718, 2024.

[19] J. Zhang, C. Peng, X. Xie, and D. Yue, "Output feedback stabilization of networked control systems under a stochastic scheduling protocol," *IEEE Transactions on Cybernetics*, vol. 50, no. 6, pp. 2851–2860, 2020.

[20] F. Tobagi, "Multiaccess protocols in packet communication systems," *IEEE Transactions on Communications*, vol. 28, no. 4, pp. 468–488, 1980.

[21] P. Cheng, G. Zhang, W. Zhang, and S. He, "Co-design of adaptive event-triggered mechanism and asynchronous $\mathcal{H}_\infty$ control for 2-D Markov jump systems via genetic algorithm," *IEEE Transactions on Cybernetics*, vol. 53, no. 9, pp. 5729–5740, 2023.

[22] Z. Zhang, Y. Niu, Z. Cao, and J. Song, "Security sliding mode control of interval type-2 fuzzy systems subject to cyber attacks: The stochastic communication protocol case," *IEEE Transactions on Fuzzy Systems*, vol. 29, no. 2, pp. 240–251, 2021.

[23] Y. Tang, X. Zhou, P. Li, J. Cao, and J. Cheng, "Sliding mode control for Markov jump singularly perturbed systems under piecewise homogeneous stochastic communication protocol," *IEEE Transactions on Cybernetics*, vol. 54, no. 7, pp. 4002–4013, 2024.

[24] J. Liu, J. Ke, J. Liu, X. Xie, and E. Tian, "Secure event-triggered control for IT-2 fuzzy networked systems with stochastic communication protocol and FDI attacks," *IEEE Transactions on Fuzzy Systems*, vol. 32, no. 3, pp. 1167–1180, 2024.

[25] Y. Yang, Y. Niu, and H.-K. Lam, "Sliding mode control for networked interval type-2 fuzzy systems via random multiaccess protocols," *IEEE Transactions on Fuzzy Systems*, vol. 30, no. 11, pp. 5005–5018, 2022.

[26] X. Li, X. Ma, W. Tai, and J. Zhou, "Designing an event-triggered $\mathcal{H}_\infty$ filter with possibly inconsistent modes for Markov jump systems," *Digital Signal Processing*, vol. 139, p. 104092, 2023.

[27] J. Zhou, J. Dong, and S. Xu, "Asynchronous dissipative control of discrete-time fuzzy Markov jump systems with dynamic state and input quantization," *IEEE Transactions on Fuzzy Systems*, vol. 31, no. 11, pp. 3906–3920, 2023.

[28] Y. Tao and Z. Wu, "Asynchronous control of two-dimensional Markov jump Roesser systems: An event-triggering strategy," *IEEE Transactions on Network Science and Engineering*, vol. 9, no. 4, pp. 2278–2289, 2022.

[29] W. Marszalek, "Two-dimensional state-space discrete models for hyperbolic partial differential equations," *Applied Mathematical Modelling*, vol. 8, no. 1, pp. 11–14, 1984.

[30] T.-S. Lee, I.-F. Chen, T.-J. Chang, and C.-J. Lu, "Forecasting weekly influenza outpatient visits using a two-dimensional hierarchical decision tree scheme," *International Journal of Environmental Research and Public Health*, vol. 17, no. 13, p. 4743, 2020.

[31] J. V. Soulis, "Computation of two-dimensional dam-break flood flows," *International Journal for Numerical Methods in Fluids*, vol. 14, no. 6, pp. 631–664, 1992.

[32] X. Li and Y. Sun, "Stock intelligent investment strategy based on support vector machine parameter optimization algorithm," *Neural Computing and Applications*, vol. 32, no. 6, pp. 1765–1775, 2020.

[33] Y. Shen, Z. Wu, P. Shi, and G. Wen, "Dissipativity based fault detection for 2D Markov jump systems with asynchronous modes," *Automatica*, vol. 106, pp. 8–17, 2019.